Retrofit modeling for green ships

Hermans, J.J.M.; Kana, A.A.

DOI
10.59490/imdc.2024.890

Publication date
2024

Document Version
Final published version

Published in
Proceedings of the 15th International Marine Design Conference (IMDC-2024)

Proceedings of 15th International Marine Design Conference (IMDC-2024)
June 2-6, 2024
Amsterdam, the Netherlands

Retrofit modeling for green ships

Julien J. M. Hermans[1] and Austin A. Kana[2,*]

ABSTRACT

This paper proposes a data-driven approach to reduce emissions in international shipping, aligning with the IMO's goal of achieving net-zero greenhouse gas emissions by around 2050. Digital twins (DTs) offer promise for maritime decarbonization due to their simulation and big data handling capabilities. However, fully realizing DTs for new-build is by definition challenging as it requires a real-time data connection. Thus, the research begins with retrofitting existing ships using operational data collected through Bunker Delivery Notes (BDNs), a mandatory method for larger ships since January 2019. The proposed framework constructs digital models to support the retrofit DT, that are tested on a 300m bulk carrier. A fuel consumption model is built using a gray box approach, while various wind-assisted ship propulsion systems are modeled using a white box approach. The study evaluates the design implications and emissions reduction potential of implementing these systems.

KEY WORDS

Retrofit; alternative power and energy; wind-assisted ship propulsion; bunker delivery notes; gray box modeling; Digital Twin for Green Shipping DT4GS.

NOMENCLATURE

ANN Artificial neural network

BBM Black box model

BDNs Bunker delivery notes

CII Carbon Intensity Indicator

DM Digital model

DS Digital shadow

DT Digital twin

DT4GS Digital Twin for Green Shipping

EEXI Energy Efficiency Existing Ship Index

FCM Fuel consumption model

GBM Gray box model

GDR Gap distance ratio

GHG Greenhouse gas

IMO International Maritime Organization

LLs Living labs

MAPE Mean absolute percentage error

WASP Wind-assisted ship propulsion

WBM White box model

[1] Delft University of Technology, Department of Maritime and Transport Technology, Delft, the Netherlands
[2] Delft University of Technology, Department of Maritime and Transport Technology, Delft, the Netherlands; ORCID: 0000-0002-9600-8669
[*] Corresponding Author: a.a.kana@tudelft.nl

Submitted: 23 February 2024, Revised: 19 April 2024, Accepted: 1 May 2024, Published: 23 May 2024

Conference paper, DOI: https://doi.org/10.59490/imdc.2024.890 e-ISSN: 3050-486

INTRODUCTION

During the United Nations Climate Change Conference near Paris in 2015, the Paris Agreement was adopted by the 196 parties present which stated that global warming must be limited to below 2°C (EC, 2015). Unfortunately, international shipping together with international aviation were not taken into account in this agreement. As a reaction, the International Maritime Organization (IMO) adopted in 2018 an initial strategy in order to reduce greenhouse gas (GHG) emissions by international shipping (IMO, 2018).

The goal of this initial strategy is set on a reduction of GHG emissions by 50% in 2050 compared to emission levels of 2008. During their annual meeting in July 2023, the strategy was revised to net-zero GHG goal close to 2050, addressing the IMO's environmental ambitions (IMO, 2023). The maritime industry generates vast amounts of data concerning vessel operations, route details, port activities, and more. Yet, much of this data remains underutilized due to factors such as manual processing and limited application beyond specific purposes like incident assessment or environmental impact measurement (Swider et al., 2018). This is due to the involvement of multiple stakeholders and the complexity of modern vessel design and operation. To address this challenge, researchers recommend focusing on research and innovation in digitalization and data usage within the shipping industry, exploring technologies such as artificial intelligence, augmented reality, virtual reality, high-performance computing, and big data analytics (Mouzakitis et al., 2023; Swider et al., 2018). These technologies hold potential for various maritime applications, including vessel traffic management, energy system design and operation, autonomous shipping, fleet intelligence, and route optimization. Despite ongoing digitalization efforts in other industries, such as aerospace and manufacturing, the maritime industry lags behind in embracing these advancements due to its complex and heavily regulated nature (Mouzakitis et al., 2023). However, leveraging shipping data has the potential to drive beneficial developments in marine engineering and propel the industry toward more digitally driven processes.

As a result of the Paris Agreement, the European Commission delivered in 2021 their European Green Deal in which they adopted a series of project proposals in order to achieve their own goal of reducing European GHG emissions by at least 55% by the year 2030, relative to 1990, and zero-net GHG emissions by 2050. By achieving this goal, the EC wants to become the first climate-neutral continent in the world, hence zero emission for international shipping (EC, 2021a,b). One of these projects is the Digital Twin for Green Shipping (DT4GS) project, funded by the European Union's Horizon research program. The goal of DT4GS is to eventually accomplish zero emissions by 2050 for the ship types of the collaborating companies within the DT4GS project; represented by an oil tanker, a container ship, a bulk carrier, and a ROPAX vessel. The collaborating vessels function as so-called 'Living Labs' (LLs), where operational data is collected to be used for improving green ship design based on digital twin (DT) methods. This research supported the DT4GS project by investigating the feasibility of a data-driven design method to reduce ship's CO_2 emissions.

WIND-ASSISTED SHIP PROPULSION

One obvious strategy regarding green shipping is the use of renewable energy, especially wind power. Due to its history with shipping and its availability at sea, the focus within renewable energy is shifting towards wind power (de Kat and Mouawad, 2019). Wind-assisted ship propulsion (WASP) systems have proven to achieve significant power reductions under favorable wind conditions: Thies and Ringsberg (2023) achieved a reduction between 10% and 14% by applying a Flettner rotor during the retrofitting of a ROPAX vessel, providing new-build design parameters for future ships with this WASP system. Bentin et al. (2018) investigated the energy-saving potential of using a towing kite, DynaRig sail, and Flettner rotor for a multi-purpose carrier, bulk carrier, and tanker. A saving potential of up to 35% was found when incorporating route optimization regarding favorable wind conditions. The investigated ship types were selected because they identified them to be suitable for WASP installation without changing the ship's capacity and the cargo loading and unloading function of the ship (Bentin et al., 2018). This is also addressed by Reche-Vilanova et al. (2021), where tankers and bulk carriers are identified to be especially suitable for WASP system installation due to their available deck space.

DEFINITION DIGITAL TWIN

In order to provide a clear explanation of the conducted research, a definition of a DT is chosen that is strictly followed during this study. Mauro and Kana (2023) identified that the term 'digital twin' is often falsely used throughout scientific research. In order to not contribute to this error in nomenclature, the model distinction adopted by Kritzinger et al. (2018) will be used throughout this research:

- A *digital model* (DM) which is a virtual representation of the physical product, but without any form of exchange of automated data between both. Data exchange could occur but only be performed manually. The DM is mostly used for simulation and planning-based operations which does not require automatic data integration.
- A *digital shadow* (DS) which is an extended version of a DM including only an automated data flow from the physical product towards the virtual product by which it is actively updated.
- And lastly a *digital twin* (DT) is, composed of a physical and virtual product including an automated data flow between both entities.

DT-SUPPORTED RETROFIT DESIGN

In order to investigate the state-of-the-art DT applications for maritime design, Mauro and Kana (2023) conducted a systematic literature review regarding maritime DT applications. Additionally, Hermans (2024) conducted a literature survey up to October 2023 for DT ship design. In these investigations, no publications are found on concrete DT applications for both new-build vessels and retrofits considering a whole vessel. Only theoretical frameworks and concepts are presented. In this research, a DT for retrofit design is investigated. First, the objective of the DT needs to be determined before starting with the actual modeling process for a DT-supported design. The objective covers the DT composition by indicating the required virtual models, and this composition consequently depends on the available data used by the final DT for performing simulations. The available operational data thus drives the modeling process of the DT (Giering and Dyck, 2021). The virtual models that are feasible to construct are identified by investigating this data. Finding the overlap between the required models (derived from the DT objective) and the feasible models (derived from the available data) provides the model selection for the final DT (see Figure 1).

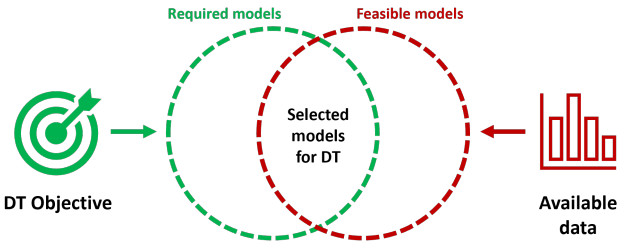

Figure 1: Selection process for DT models (Hermans, 2024)

After establishing the DT's objective and the model selection process, the modeling phase involves the following general steps, where the details can be found in Hermans (2024) and Papanikolaou et al. (2024):

1. Set-up the data acquisition
2. Choose modeling approaches for virtual models
3. Perform model training in case of statistical-based models
4. Integrate the virtual part with the physical part

Figure 2 shows a schematic representation of the transition towards a DT for retrofitting, where a detailed description can be found in Hermans (2024) and Papanikolaou et al. (2024).

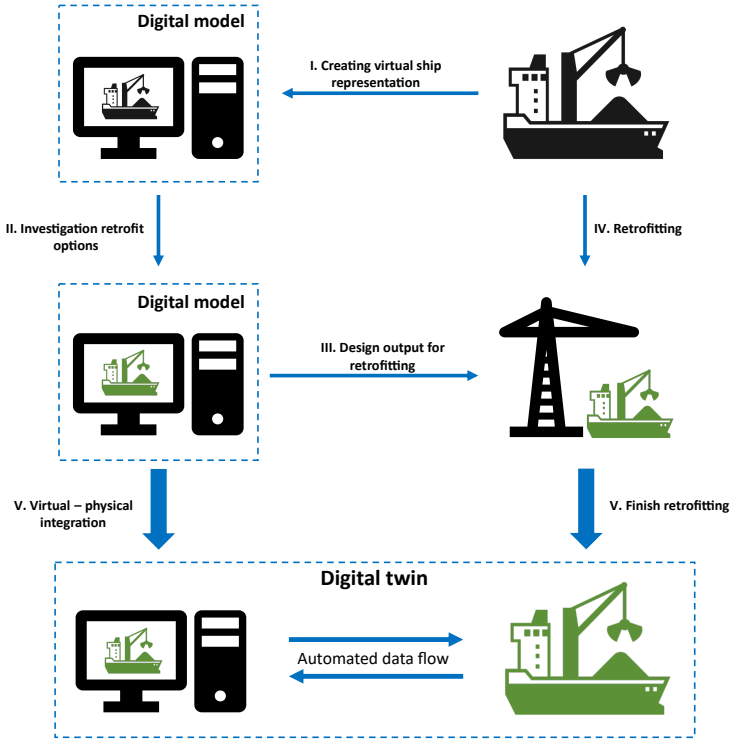

Figure 2: The development of the digital twin for retrofitting, based on the adopted DT definition (Hermans, 2024)

CONDUCTED RESEARCH

A DT with a retrofit design purpose starts as a digital model which becomes a DT after the retrofitting is completed. This research focuses on the modeling of the virtual part within the DT environment which will lay the basis for a green ship DT using this operational ship's data. Thus, using the definition by Kritzinger et al. (2018), this research will work on a green ship DM, supporting the process of constructing the DT (Figure 3).

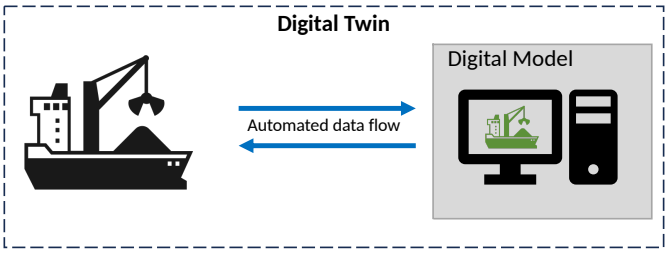

Figure 3: Focus of this research: representation of the green ship digital model (gray) within final digital twin

For the modeling construction, a model that represents the ship and a model that represents the green ship technologies are developed, which ultimately are integrated into one green ship DM. Within the DT4GS project, bunker delivery notes (BDNs) of a 300m bulk carrier are available as the data source. The main DT objective is set to reduce CO_2 emission through ship design, for which the Energy Efficiency Existing Ship Index (EEXI) and the Carbon Intensity Indicator (CII) are used

to evaluate this objective. The EEXI and CII are both IMO's environmental measurement tools which have been mandatory for most transport vessels since January 2018. Using these principles, the model selection (Figure 1) resulted in a fuel consumption model (FCM) which represents the ship, and three WASP models (towing kite, DynaRig sail, Flettner rotor), which represent the green ship technologies. The FCM will be composed of a resistance model and an artificial neural network (ANN). The resistance model will be modeled as a white box model (WBM), and the ANN as a black box model (BBM). Both are connected in a serial coupled fashion which results in an FCM constructed as a gray box model (GBM). The WASP models are all three modeled as WBMs. By combining these models into one green ship DM a potential retrofit design can be examined (Figure 4).

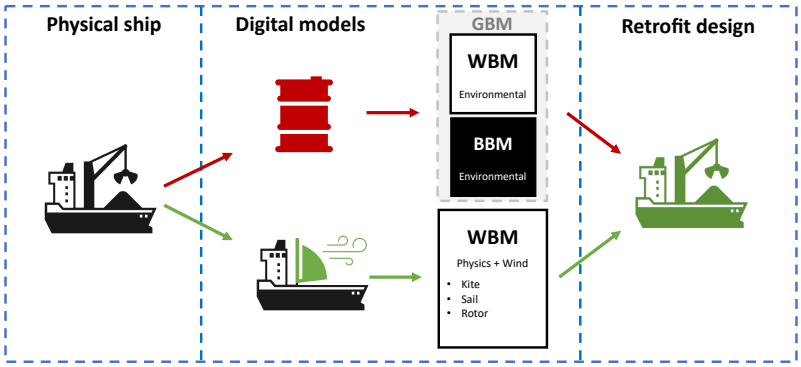

Figure 4: Overview of chosen method for constructing green ship DM. Combination of part representing the ship (red oil barrel) and part representing green ship technologies (green wind sail) resulting in one green ship DM for retrofit design (green bulk carrier)

A 300-meter bulk carrier is used as the case-study to investigate the proposed data-driven design approach. Besides evaluating the environmental impact of the EEXI and CII, a financial and feasibility assessment will be performed to investigate if the proposed retrofit of the respective vessel can be achieved. The payback period functions as the financial assessment. During the selection of WASP system configurations, the spatial feasibility per configuration is evaluated.

DATA PREPROCESSING

The available BDNs of the bulk carrier contain over 129,000 data points, with a time interval of 5 minutes during the following periods:

- Q2 2022: 02/06/'22 - 30/06/'22
- Q3 2022: 01/07/'22 - 30/09/'22
- Q4 2022: 01/10/'22 - 31/12/'22
- Q1 2023: 01/01/'23 - 24/02/'23
- Q2 2023: 01/04/'23 - 30/06/'23
- Q3 2023: 01/07/'23 - 30/09/'23

The abundance of operational data from the BDNs does not necessarily imply that all these data are of good quality and in the right format to be utilized. In order to be of use for the case-study, the data is first preprocessed. Figure 5 shows the steps performed within the adopted data preprocessing framework of this research. These preprocessing steps are based on the techniques described by García et al. (2016).

For the case study, only data points corresponding to sailing conditions of the ship are considered, with a minimum ship speed of 6 knots through water selected to filter out non-sailing data points during the data selection process (step 2). During the noise identification (step 3), outliers within the dataset are identified, as they can negatively impact the accuracy of the models if left untreated. To address this issue, outliers are either replaced through interpolation around the respective

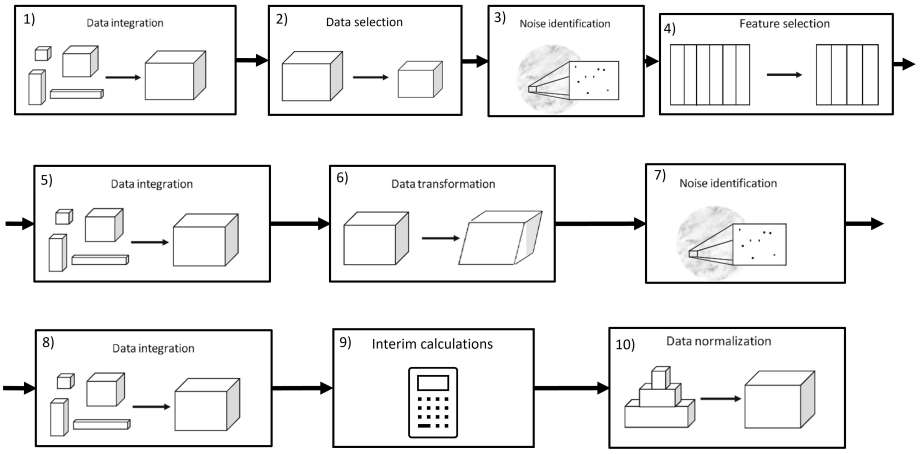

Figure 5: Adopted preprocessing data framework, based on techniques by García et al. (2016) (Hermans, 2024)

data points or entirely disregarded. In this research, identified outliers are simply disregarded. The following criteria are used during the noise identification process:

- Brake power is negative or zero
- The instant specific fuel consumption of the main engine is negative or zero (a result of a calculation)
- Sampling time is not 5 minutes
- Speed through water difference between 2 data points (= 5 min) is more than 3 knots, the second point is then disregarded

The other preprocessing steps within the adopted framework are discussed more thoroughly in Hermans (2024). The resulting amount of data points reduced per preprocessing step is provided in table 1. After performing the adopted data preprocessing steps, 5,687 data points remained. However, inspecting the resulting data points per period, significant anomalies were observed in Q2 2022, resulting in only 9 useful sailing hours. These 9 hours are just a tiny fraction of the resulting 5,687 hours (0.2%) and are therefore disregarded. This results in 5,678 data points, representing 'pure' sailing conditions, to be used for model construction.

Table 1: Data preprocessing results of BDNs data

	Data integration	Data selection	Noise identification				Data transformation
Period	Raw	$V_s \geq 6$ kts	$sfc_{ME} \leq 0$	$P_B \leq 0$	$T_s \neq 5$ min	$\Delta V_s \geq 3$ kts	Hour conversion
Q2 2022	8,267	3,165 (-5,102)	2,769 (-396)	148 (-2,621)	148 (0)	147 (-1)	9 (-39)
Q3 2022	26,488	15,582 (-10,906)	15,579 (-3)	15,572 (-7)	15,572 (0)	15,570 (-2)	1,284 (-162)
Q4 2022	26,493	18,281 (-8,212)	18,280 (-1)	18,280 (0)	18,279 (-1)	18,276 (-3)	1,514 (-108)
Q1 2023	15,697	9,756 (-5,941)	9,756 (0)	9,756 (0)	9,756 (0)	9,755 (-1)	802 (-131)
Q2 2023	26,207	12,586 (-13,621)	12,586 (0)	12,586 (0)	12,586 (0)	12,586 (0)	1,047 (-22)
Q3 2023	26,022	13,404 (-12,618)	13,353 (-51)	12,647 (-706)	12,645 (-2)	12,641 (-4)	1,031 (-269)
Σ	129,174	72,774 (-43.7%)				68,975 (-5.2%)	5,687 (-1.1%)

MODEL CONSTRUCTION

Fuel consumption model - GBM

Resistance model - WBM

The resistance model calculates the sum of the ship's calm water resistance (R_{cw}), according to the Holtrop and Mennen (1982), and the wind resistance (R_{AA}) using the method of Andersen (2013). The available sea trial report provides 6 runs with which the output of the resistance model can be verified. The R_{cw} and R_{AA} for each of these runs is calculated and compared with the measured value during the run. The mean errors from this comparison are listed in Table 2. The ship had a course direction of $60°$ during runs 1 to 3, and a course direction of $240°$ during runs 4 to 6.

Table 2: Mean percentage error resistance. Run 1 to 3 with course direction $\Psi = 60°$, run 4 to 5 with course direction $\Psi = 240°$

Resistance	Run 1	Run 2	Run 3	Run 4	Run 5	Run 6
$\Sigma(R_{cw} + R_{AA})$	+10.0%	+12.1%	+20.5%	-7.2%	-0.0%	+7.5%
R_{cw}	+12.9%	+14.4%	+24.2%	-7.1%	-0.0%	+7.6%
R_{AA}	-0.4%	-0.0%	-0.4%	-1.8%	-0.4%	+0.7%

As it can be noticed, the resistance prediction with a course direction of 240° is more accurate than the 60°. Moreover, the prediction of the additional wind resistance has a maximum error of 1.8%. The prediction of the calm water resistance fluctuates the most but within a 15% error when indicating run 3 as an outlier. There is no explanation found for the resistance difference between the two course directions and the relatively high error of run 3. The overall mean absolute percentage error is 9.6% which is deemed acceptable.

Artificial neural network - BBM

The ANN is constructed with Keras, which is an open-source neural network API written in Python (v3.11.5) that runs on top of the TensorFlow library (Keras, 2023). Before determining the architecture of the ANN, model inputs are chosen from the available data in the BDNs. The BDNs contain over 100 different data types. To ensure the accuracy and representativeness of fuel consumption predictions for future scenarios, an initial selection is made of potential model input parameters. This selection is based on the following assumptions:

- The goal is to predict fuel consumption with an operating WASP system, which will influence engine characteristics in a way that is currently unknown. Thus, parameters strongly related to the operating engine are left out of consideration
- Environmental parameters can be predicted for future situations by means of weather models, and are therefore taken into account
- Voyage characteristics such as ship speed and rudder position are route-dependent and can be chosen for future voyages

Following this filtering process, 12 potential model input parameters are identified. To refine the selection further, a Spearman correlation analysis is conducted for these parameters, specifically focusing on their correlation with the fuel consumption of the main engine. The analysis results, presented in Table 3, guide the final input selection process. Notably, in terms of engine output, engine torque is disregarded in favor of selecting brake power, as both parameters exhibit similar correlation factors, and power is deemed more suitable for WASP implementation.

Table 3: Spearman correlation for determination ANN inputs

Data types	Correlation with fuel consumption main engine	Selection
Brake power output	0.787	✓
Engine torque output	0.789	✗
Ship's heading	-0.082	✗
Rudder angle	-0.241	✓
Rudder rate of turn	0.002	✗
Relative wind direction	0.131	✓
Relative wind speed	0.226	✓
Speed over ground	-0.068	✗
Speed through water	0.142	✓
Speed difference	-0.170	✓
Total power diesel generators	0.041	✗
Sea water temperature	-0.174	✓
Fuel consumption main engine	1.000	—

From the Spearman correlation analysis, 7 parameters from the BDNs are chosen as model inputs. Additionally, the output of the resistance model, $\Sigma(R_{cw} + R_{AA})$, is incorporated as an additional input, which results in a total 8 model inputs for the ANN. This inclusion of the resistance as ANN input gives the model its gray box characteristic, and in this case, serially coupled. The 8 model inputs are:

- Brake power output
- Rudder angle
- Relative wind direction
- Relative wind speed
- Speed through water (ship speed)
- Speed difference
- Sea water temperature
- Sum of calm water and air resistance (result WBM)

The resulting 5,678 data points from the preprocessing are used for constructing the ANN. Initially, 500 data points are randomly selected for later cross-validation (referred to as the test set), leaving 5,178 points for training and intermediate validation to determine the optimal ANN architecture. These remaining data points are divided into a training set and a validation set at a ratio of 90% - 10%. The division is made using a specified random state (*rs*) parameter. During training, the weights of neurons are adjusted using the training set, while the validation set is used to monitor the ANN's loss.

The majority of research on ANNs for fuel consumption prediction suggests using a single hidden layer to balance complexity and accuracy (Hu et al., 2019; Bal Beşikçi et al., 2016). However, some studies propose the use of multiple hidden layers for improved prediction accuracy (Parkes et al., 2018; Fam et al., 2022). The accuracy of the ANN is closely tied to the number of hidden layers and neurons, with more units allowing for the modeling of complex relationships (Parkes et al., 2018). Nevertheless, networks with too few layers and neurons may struggle to capture all necessary relationships effectively. To address this, both one and two hidden layer configurations are explored, using the Fletcher-Gloss method described in da Silva et al. (2017) to determine the number of neurons. This resulted in 209 potential configurations of which the resulting configuration was chosen (Figure 6). The final ANN characteristics and training parameters are listed in Table 4. The choice and background of the training parameters are discussed more thoroughly in Hermans (2024).

The resultant ANN configuration with the highest accuracy is a network with 1 hidden layer containing 16 neurons. Three additional networks with the same configuration (1 hidden layer of 16 neurons) are constructed for cross-validation, each using a different *rs* value during training to yield networks with different weights per neuron. These networks are cross-validated using a test set of 500 data points that were set aside, ensuring that the achieved accuracy is independent of the specific data split used for training. The mean absolute percentage error (MAPE) for each network is listed in Table 5, along with the overall MAPE and corresponding standard deviation.

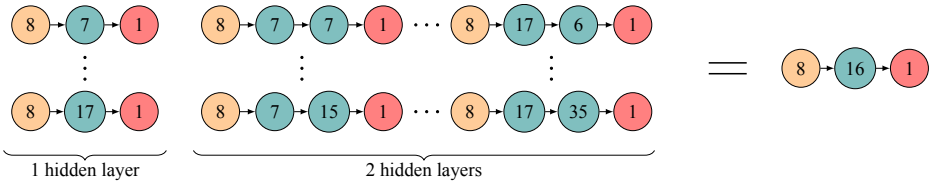

Figure 6: Investigated ANN configurations with 1 input layer (yellow), 1 or 2 hidden layers (green), and 1 output layer (red) (Hermans, 2024)

Table 4: ANN characteristics and training parameters

Characteristic - parameter	Value
Training algorithm	Adam
Activation function	ReLU
Number of inputs	8
Number of outputs	1
Number of hidden layers	1
Neurons in hidden layer	16
Dropout	0.2
Test set	500 data points
Training - validation set	90% - 10%
Batch size	16 data points
Max number of epochs	500
Learning rate	0.001
Patience	35 epochs
Monitor loss function	MSE

Table 5: Cross-validation using test data set between 4 models with equal configuration

Random state	MAPE
49	1.8%
59	2.1%
61	1.9%
80	1.9%
Overall	1.9%
Standard deviation	+/- 0.1%

The confidence interval is a common practice in statistics to indicate if the adopted method is within a desired accuracy (Carney et al., 1999). The minimum desired confidence interval for machine learning, and especially ANNs, is generally 90% (Carney et al., 1999). The constructed ANN is well within this interval, with an overall MAPE of 1.9% indicating the high accuracy of the network.

WASP models

In this research three distinctive WASP system models are constructed: a towing kite, a DynaRig sail, and a Flettner rotor. The selection for the towing kite and DynaRig sail is based on available literature (Bentin et al., 2018; Reche-Vilanova et al., 2021) on these models that use wind data that corresponds with the available data in the BDNs. Within the DT4GS project, a digital model of a Flettner rotor is constructed by Witzgall (2023) which is used in this research.

Wind conversion

The wind sensor which measures the wind speed and direction found in the BDNs is mounted on the mast on the bridge deck. As the wind profile is not constant over the height, the wind speed needs to be converted to the corresponding effective height of the respective WASP system. This conversion is calculated with Equation 1, which represents the power-law of the wind profile (Hsu et al., 1994).

$$V_{z_{WASP}} = V_{z_{measured}} \cdot \left(\frac{z_{WASP}}{z_{measured}} \right)^{P} \tag{1}$$

The power-law exponent (P) is a spatial parameter depending on the surroundings of the specific situation (e.g., at sea, open or undulating terrain). Hsu et al. (1994) concluded from their experiments that an exponent of $P = 0.11$ is an accurate approximation for the wind profile over the sea. This is also in line with the recommended procedures and guidelines provided by the ITTC (2021) concerning this wind speed conversion.

Towing kite - WBM

The constructed model is based on the research of Bentin et al. (2018). The resultant propulsion force by the towing kite is approximated with Equation 2.

$$F_{kite} = 0.5 \epsilon \rho_a V_a^2 S_{wi} F_{norm,kite} \tag{2}$$

The relative wind speed (V_a) acts on the effective wind surface of the kite (S_{wi}). Here $F_{norm,kite}$ is the normalized propulsion force of the towing kite as a function of only the relative wind direction and elevation angle (δ), and can be calculated with Equation 3.

$$F_{norm,kite} = \left(\cos\left(\frac{180^\circ - \varphi_{a,rel}}{2} \right) \right)^2 \cdot (\cos(\delta))^2 \tag{3}$$

Four kite configurations were investigated during the case-study, referred to as: *Kite300*, *Kite800*, *Kite1280* and *Kite2500*. These configurations vary in kite sail area, which are respectively: 300 m^2, 800 m^2, 1,280 m^2 and 2,500 m^2. The characteristics per kite configuration are listed in Table 6. It is assumed that the kite system is a fully autonomous system, including kite deployment and retrieving. An electric motor, included in the kite system, controls the flight and logistics. Such a fully autonomous system is also considered in the book chapter by Fritz (2013). The power usage of the electric motor is estimated at 2 kW with an electric efficiency of 0.95.

Table 6: Towing kite configurations

Kite characteristic	Kite300	Kite800	Kite1280	Kite2500
Kite sail area [m^2]	300	800	1,280	2,500
Height [m]	77.6	150	250	400
Elevation angle [°]	15	30	30	30

DynaRig sail - WBM

As with the kite model, the DynaRig sail model is also based on the modeling methods described by Bentin et al. (2018), together with the research conducted by Reche-Vilanova et al. (2021). The resultant propulsion force by the sail is calculated

with Equation 4. Here, the sail surface is represented by A_S. The normalized propulsion force $F_{norm,sail}$ is derived from the relative wind angle $\varphi_{a,rel}$ and the lift and drag coefficients (C_L and C_D). These coefficients characterize a specific sail. $F_{norm,sail}$ is calculated with Equation 5.

$$F_{sail} = 0.5 A_S \rho_a V_a^2 F_{norm,sail} \tag{4}$$

$$F_{norm,sail} = C_L \sin(\varphi_{a,rel}) - C_D \cos(\varphi_{a,rel}) \tag{5}$$

Bordogna (2020) conducted wind tunnel tests for 3 different DynaRig sail configurations and only investigated the lift and drag coefficients of the respective sail without interaction effects. For this reason, the derived force coefficients by Bordogna (2020) are used for this DynaRig model. The sails were virtually trimmed during Bordogna's experiments to optimize for the maximum thrust per apparent wind angle. During the experiments 3 different sail configurations are investigated: 1 sail, 2 sails with a gap distance ratio (GDR) of 2.5, and 2 sails with a GDR of 4. The GDR is defined as the ratio of the distance between two sails and the chord length of a sail. These configurations will be referred to as *DynaRig single*, *DynaRig double 2.5*, and *DynaRig double 4*. The resultant configurations are listed in Table 7, where the dimensions are determined based on the characteristics of the conducted experiments and the available spatial feasibility of the bulk carrier.

Table 7: DynaRig sail configurations

Sail characteristic	Single	Double 2.5	Double 4
Gap distance ratio [-]	-	2.5	4
Chord length [m]	20	20	12.5
Height sail [m]	37.1	37.1	23.2
Camber [%]	10	10	10

Flettner rotor - WBM

Unlike with the kite and DynaRig model, an already constructed model of a Flettner rotor adopted by Witzgall (2023) will be used. In collaboration with the DT4GS project, Witzgall (2023) used a non-linear regression method to develop a surrogate rotor model based on 7 distinctive studies conducted in the field of Flettner rotor lift and drag coefficients. Two rotor configurations are investigated: the installation of 1 rotor and 4 rotors. The configuration of 4 rotors consists of four times the same rotor as used for the configuration of 1 rotor. The goal of this research is to reduce the CO_2 emissions (i.e., fuel consumption), thus the largest feasible rotor available in the industry is selected to be investigated: a 35m high rotor with a diameter of 5m and an endplate with a diameter of 10m. Both configurations are referred to as *1x Rotor H35D5* and *4x Rotor H35D5*.

MODEL INTEGRATION

The goal of the green ship DM is to calculate the fuel consumption in case of an operating WASP. Comparing this with the fuel consumption without a WASP results in potential fuel reduction which provides an insight into the WASP's environmental and financial benefits. The output of the WASP's WBMs is propulsion force and possible power demand. One of the inputs of the ANN in the FCM is the ship's brake power. Thus, the ship's brake power including WASP force needs to be determined while maintaining the same ship speed and sailing time. The WASP's propulsion force is implemented with the propeller thrust demand in the ship's force balance to overcome the experienced resistance. This force balance is represented by Equation 6. Using this force balance a new working point of the propeller is derived, which is also known as the propeller-matching procedure. Vigna and Figari (2023) have performed this matching procedure including an operating Flettner rotor in order to derive the ship's brake power. The adopted integration framework is based on this procedure. The

ship speed and sailing time are kept the same as only the influence on the ship's brake power by the installed WASP system is being considered.

$$\underbrace{R_T = (1-t)\cdot T}_{\text{Without operating WASP}} \quad \Rightarrow \quad \underbrace{R_T = (1-t)\cdot T + F_{WASP}}_{\text{Including operating WASP}} \tag{6}$$

Equation 6 is rewritten to the forward equilibrium equation including the terms of the propeller characteristics and hull demand resulting from the required ship speed, to derive the new working point of the propeller (Vigna and Figari, 2023), resulting in Equation 7.

$$\underbrace{\frac{K_T}{J^2} - \frac{R_T}{\rho_{sw}\cdot(1-t)(1-w)^2\cdot V_s^2\cdot D_p^2} = 0}_{\text{Without operating WASP}} \quad \Rightarrow \quad \underbrace{\frac{K_T}{J^2} - \frac{R_T - F_{WASP}}{\rho_{sw}\cdot(1-t)(1-w)^2\cdot V_s^2\cdot D_p^2} = 0}_{\text{Including operating WASP}} \tag{7}$$

The established model integration framework for this research is depicted in Figure 7. The output of the WASP WBMs is firstly transformed into brake power, and next integrated into the FCM to predict the corresponding fuel consumption. The required steps for this integration are depicted in orange and are discussed in Hermans (2024). This presented framework is based on evaluating the known data from the BDNs. Necessary calculation adjustments in this framework for future data sets are also presented in Hermans (2024).

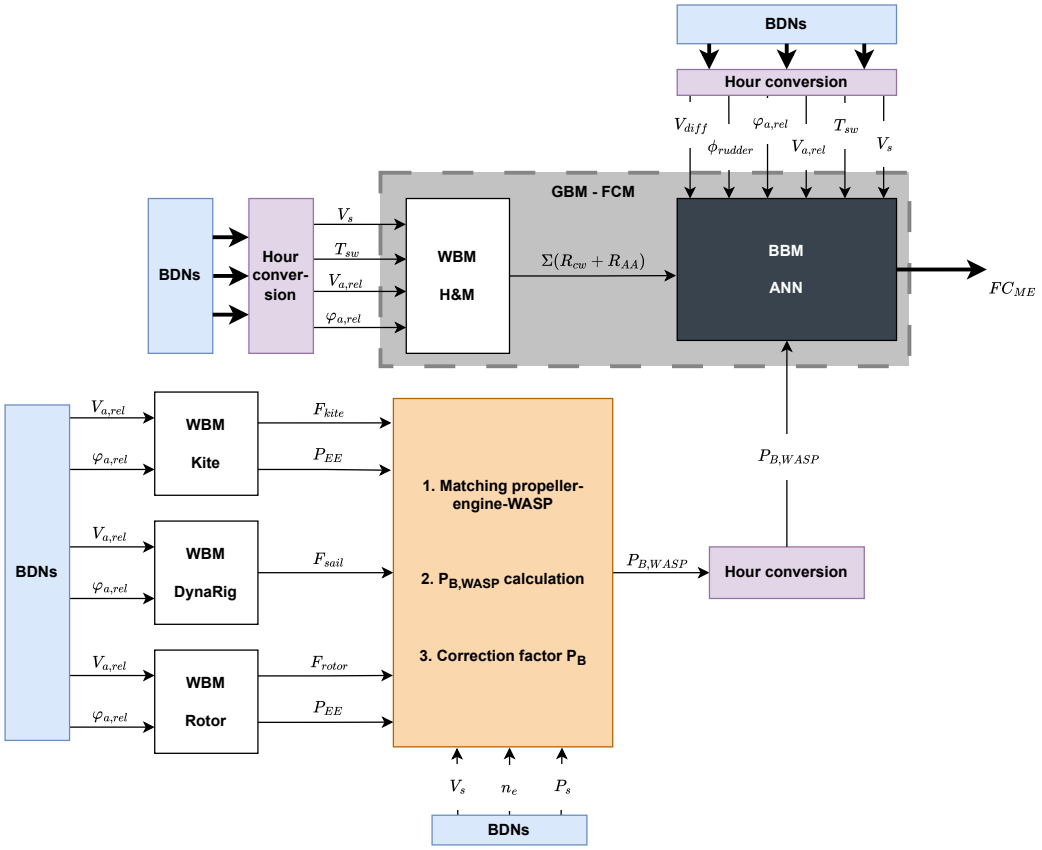

Figure 7: Schematic overview digital models including, the adopted model integration framework in orange (Hermans, 2024)

Step 3 in the integration framework (Figure 7) consists of a correction factor (*cf*) calculation of the ship's brake power. Because the current brake power is recorded in the BDNs, this *cf* can be calculated per data point to improve accuracy in the power computation. This *cf* can be seen as a variable value for all the efficiencies used in the brake power calculation (i.e., $\eta_S, \eta_{GB}, \eta_R$). The ship's forward equilibrium equation without operating WASP (in Equation 7), together with the derivation for the brake power (Equation 8) using the BDNs is used to calculate the ship's brake power. Because the bulk carrier does not have a gearbox, the propeller rotation (n_p) is assumed to be equal to the measured main engine rpm (n_e) available in the BDNs. This calculated value is compared with the measured brake power (BDNs) to derive the *cf* per data point (Equation 9). The correction factor is then multiplied by the ship's brake power with operating WASP.

$$P_B = \frac{2\pi\rho_{sw} D_p^5 n_p^3 K_Q}{\eta_S \eta_{GB} \eta_R} \tag{8}$$

$$cf = \frac{P_B \text{ (BDNs)}}{P_B \text{ (calculated)}} \tag{9}$$

RESULTS

Overall savings Q3 2022 - Q3 2023

For each configuration of the WASP systems, the money, fuel, and CO_2 savings are calculated over the 5,678 sailing hours ($\approx$ 237 sailing days) using a fuel price of \$618.50/mt-fuel. These results are presented in Table 8. Percentage reductions apply to all listed savings, as they are all directly linked to fuel consumption. The savings are computed as the difference between the predicted fuel consumption by the green ship DM with and without the WASP system. The MAPE between the actual fuel consumption (BDNs) and the predicted consumption (green ship DM), both without installed WASP, is 0.3%, indicating high model accuracy and reliability. This supports the validity of using the model. Calculating the difference between both predicted values by the green ship DM ensures consistency in accuracy.

Table 8: Total WASP savings during 5,678 sailing hours

WASP configuration	Fuel savings [mt]	\$-savings [K\$]	CO_2 savings [mt]	Percentage savings [%]
Kite300	1,031	637	3,240	-12.5
Kite800	1,048	648	3,293	-12.7
Kite1280	1,070	662	3,364	-13.0
Kite2500	1,129	698	3,549	-13.7
DynaRig single	1,145	708	3,599	-13.9
DynaRig double 2.5	1,148	710	3,610	-14.0
DynaRig double 4	1,068	660	3,357	-13.0
1x Rotor H35D5	1,197	740	3,762	-14.6
4x Rotor H35D5	1,598	989	5,025	-19.4

The overall results indicate a CO_2 reduction potential ranging from 12% to 19% across the investigated WASP configurations. This finding aligns with a literature study conducted by Bouman et al. (2017) on CO_2 reduction through green ship technologies, who found savings potentials between 7% and 22% of similar WASP technologies. When comparing individual configurations of each WASP system (1 kite, 1 sail, 1 rotor), it is observed that the rotor configuration offers the most significant savings potential. Additionally, kite configurations demonstrate progressively increasing savings potential with larger kite sail areas. Variations in the savings potential between the two double DynaRig configurations are attributed to differences in sail sizes as discussed in the WASP model construction.

Environmental assessment

EEXI

The power reduction due to an operating WASP is calculated according to the procedure presented in IMO (2021). Examining the sailing route of the bulk carrier during the period Q3 2022 - Q3 2023 showed that the vessel had sailed approximately 90% on the same shipping routes on which the IMO's wind probability matrix is based. This indicates that this wind prediction method, used in the EEXI calculation, has sufficient accuracy regarding this ship's operational area. The ship's current, required, and resulting EEXI values per investigated WASP configuration are provided in Table 9.

Table 9: New EEXI value per installed WASP configuration

WASP configuration	EEXI [g/(mt-nm)]	Reduction [%]
Required value (max)	2.370	-
No WASP (current)	2.120	-
Kite300	2.112	-0.4
Kite800	2.101	-0.9
Kite1280	2.085	-1.6
Kite2500	2.044	-3.6
DynaRig single	2.054	-3.1
DynaRig double 2.5	2.052	-3.2
DynaRig double 4	2.095	-1.2
1x Rotor H35D5	2.029	-4.3
4x Rotor H35D5	1.754	-17.2

All the investigated WASP configurations decrease the ship's EEXI value as suspected and consequently comply with the required EEXI value. Moreover, as noticed with the aforementioned overall savings, installing a rotor results in the highest CO_2 reduction. The *4x Rotor H35D5* configuration is simply a factor 4 environmental beneficial in terms of design potential, as the result of the calculation by the IMO.

CII

The evaluation of the ship's operational aspect involves calculating the CII. However, there are data gaps and errors in the data for March 2023 and in the period Q3 2023, rendering the CII calculation for those periods unreliable. As the CII calculation requires a complete calendar year, it cannot provide the official CII value. Nevertheless, the calculation is performed with the data of 11 consecutive months (Q3 2022 - Q2 2023) which still offers a useful indication of the vessel's operational impact. The required CII values for the years 2023, 2024, and 2025 for the specific bulk carrier used are illustrated in Figure 8.

For the calculations of the attained CII per installed WASP configuration, a fuel oil density of 0.8352 g/cm^3 is used. The fuel consumption is predicted with the constructed green ship DM. The results are provided in Table 10, including color labeling per CII corresponding to its rating for the year 2023.

The bulk carrier is currently above the required CII, in the C-rating. All the WASP configurations bring the bulk carrier in the B-rating regarding the year 2023, whereas both rotor configurations also comply with the B-rating regarding the year 2024 and *4x Rotor H35D5* extend B-compliance for the year 2025.

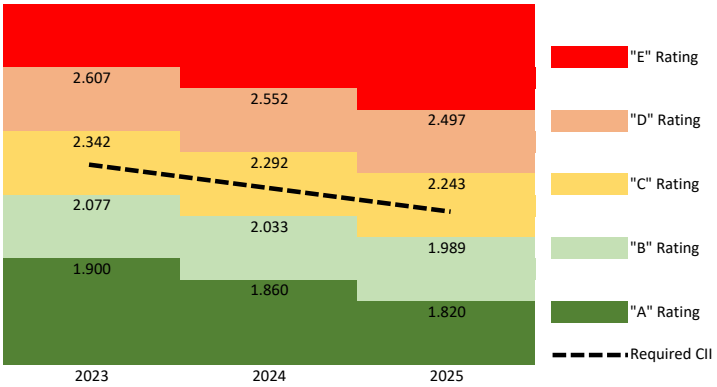

Figure 8: Attained CII values of the investigated bulk carrier; required CII values for 2023, 2024, and 2025 are respectively 2.212, 2.166, 2.119

Table 10: CII approximation of 11 months during Q3 2022 - Q2 2023

WASP configuration	Attained CII [g/(mt-nm)]
Required (2023)	2.212
No WASP	2.248
Kite300	2.059 (-8.4%)
Kite800	2.056 (-8.6%)
Kite1280	2.051 (-8.8%)
Kite2500	2.039 (-9.3%)
DynaRig single	2.035 (-9.5%)
DynaRig double 2.5	2.035 (-9.5%)
DynaRig double 4	2.052 (-8.8%)
1x Rotor H35D5	2.020 (-10.2%)
4x Rotor H35D5	1.931 (-14.1%)

Financial assessment - payback period

Even though the main objective is directly related to the environmental assessment, the financial assessment is done to give an idea of the feasibility in terms of time and money. The calculation of the payback period calculation per WASP configuration is performed with Equation 10, which is based on the financial assessments by Kiran (2022); van der Kolk et al. (2019).

$$P = \frac{B + C}{A - D} \tag{10}$$

Where the financial parameters represent:

A: $-savings per sailing hour using WASP

B: Purchase & installation system

C: Out of service costs & dry docking

D: Hourly operational & maintenance costs WASP

The $-savings per hour is the driving parameter (A) of the payback period. This parameter for each of the investigated WASP configurations (A) is derived by dividing its respective money savings in Table 8 by the total sailing hours (5,678 hrs). For the purchase and installation costs (B), the estimations provided by GloMEEP (2019) are used. GloMEEP is an international collaborating project established within the IMO aiming to support and provide insights into implementing energy-efficient measures for global shipping. Costs 'C' are not considered as there is no evident information available on these costs. This is mainly due to the fact shipping companies and maintenance docks only provide such information through a direct offer. The costs associated with the operations and maintenance of WASP systems are typically provided by the manufacturer. In this research, these costs are estimated to be annually equivalent to 2% of the WASP installation costs. This estimation aligns with a study conducted by van der Kolk et al. (2019), which performed a technological and economical assessment of WASP systems for transport vessels.

The payback period (P) for each WASP configuration can be calculated based on operational data, excluding costs 'C'. The results are presented in Table 11, considering the vessel in operational condition (minimum ship speed of 6 knots). To determine the total payback period accounting for all configurations, one must include the term $\frac{C}{A}$ to the provided payback period results, where 'C' represents the known value for costs and 'A' represents the annual savings.

Table 11: Payback period (P) of WASP configurations expressed in operating time, without costs 'C'

WASP configuration	P [hrs]	P [days]	P [years]
Kite300	4,091	170	0.5
Kite800	10,121	422	1.2
Kite1280	15,596	650	1.8
Kite2500	22,128	922	2.5
DynaRig single	1,368 $\sim$ 2,419	57 $\sim$ 101	0.2 $\sim$ 0.3
DynaRig double 2.5	2,735 $\sim$ 4,850	114 $\sim$ 202	0.3 $\sim$ 0.6
DynaRig double 4	2,943 $\sim$ 5,220	123 $\sim$ 218	0.3 $\sim$ 0.6
1x Rotor H35D5	5,437 $\sim$ 7,411	227 $\sim$ 309	0.6 $\sim$ 0.8
4x Rotor H35D5	16,696 $\sim$ 21,702	696 $\sim$ 904	1.9 $\sim$ 2.5

Analyzing the payback periods of the selected configurations indicates that the *Kite2500* and *4x Rotor H35D5* configurations require the longest time to become financially profitable. On the other hand, DynaRig configurations are generally the most favorable option in terms of payback period, averaging better results compared to other configurations.

CONCLUSION

Incorporating operational data into ship design through a DT-supported method allows for the evaluation of environmentally friendly ship designs, particularly focusing on reducing CO_2 emissions with WASP systems. The DT's capacity to handle vast amounts of data and conduct virtual simulations mitigates risks associated with such designs. Operational data from the IMO's mandatory BDNs serves as a valuable source for modeling construction, facilitating the development of a green ship DM. This DM incorporates ship characteristics, route-dependent factors, and environmental data to predict fuel consumption with and without a WASP system installed, thus estimating potential CO_2 emission reductions (environmental) and payback periods (financial). Environmental assessments conducted through IMO's EEXI and CII tools highlight the *4x Rotor H35D5* configuration as yielding the highest CO_2 reduction, while also with the longest payback time. Conversely, DynaRig configurations result as the most financially attractive on average, although dry-docking and out-of-service costs are not taken into account. Ultimately, ship owners' decisions will be guided by specific requirements and considerations, informed by the presented results.

DISCUSSION

The research focuses on integrating operational data into retrofit design, using high-level WASP models. However, these models are simplified, such as approximating aerodynamics in the towing kite model with a single value, the wind energy transfer efficiency (ϵ). To enhance the accuracy of propulsion force predictions, more refined WASP models are recommended. One key assumption is regarding fuel consumption prediction by the green ship DM with an operating WASP system. The FCM is validated with high accuracy for known sailing conditions, with one input being the ship's brake power. During the case-study, only the brake power value is altered to investigate the effect of an installed WASP system, assuming the resulting fuel consumption corresponds to that situation. To verify this assumption accurately, model or full-scale tests including WASP system installation are necessary. These tests would close the verification loop of the proposed method. The BDNs serve as a feasible data source for the modeling construction chosen in this research, providing ample data points related to route-dependent and environmental information for fuel prediction. However, there is a lack of information regarding the method and quality of the sensors used for data collection, raising uncertainty about potential errors within these values due to sensor sensitivity or recording methods. Additionally, despite the variety of recorded data types, important parameters such as waves, trim, and draft are absent. Incorporating these data types into the constructed resistance model could improve the estimation of the ship's resistance and total resistance. Although water depth data, which can influence speed loss due to shallow water effects, are present in the BDNs, they are incomplete and contain significant anomalies, leading to their exclusion from the research. Moreover, no interaction effects are considered regarding the WASP systems and the vessel during this research. While the IMO's calculations overlook these effects, deeming them significant only during unsafe operations that need to be prevented, they must be considered when investigating WASP retrofitting. The change in the center of gravity due to installing WASP systems can lead to differences in the power reduction prediction (Thies and Ringsberg, 2023). Moreover, induced trimming moments and heel angles as a result of operation WASP systems negatively influence the aero and hydrodynamic performance of the vessel's propulsion system (Smith et al., 2013; Stark et al., 2022).

DECLARATION OF GENERATIVE AI AND AI-ASSISTED TECHNOLOGIES IN WRTITING

During the preparation of this work, the authors used "OpenAI's ChatGPT 3.5" in order to guide the summarizing of several sections originating from the lead author's academic thesis. After using this tool, the authors reviewed and edited the content as needed and take full responsibility for the content of the publication.

CREDIT AUTHORSHIP CONTRIBUTION STATEMENT

Julien J. M. Hermans: Conceptualization; methodology; formal analysis; writing – original draft; writing – review and editing. **Austin A. Kana:** conceptualization; supervision; writing – review and editing.

ACKNOWLEDGEMENTS

This work was performed as part of the academic thesis for the lead author, (Hermans, 2024). The thesis was performed in Marine Technology at Delft University of Technology and the authors would like to acknowledge Delft University of Technology for their support of this research. The research also acknowledges the support by the European Union's Horizon research project DT4GS (Grant Agreement No 101056799).

REFERENCES

Andersen, I. (2013). Wind loads on post-panamax container ship. *Ocean Engineering*, 58:115–134.

Bal Beşikçi, E., Arslan, O., Turan, O., and Ölçer, A. (2016). An artificial neural network based decision support system for energy efficient ship operations. *Computers Operations Research*, 66:393–401.

Bentin, M., Kotzur, S., Schlaak, M., Zastrau, D., and Freye, D. (2018). Perspectives for a wind assisted ship propulsion. *International Journal of Maritime Engineering*, Vol 160.

Bordogna, G. (2020). Aerodynamics of wind-assisted ships : Interaction effects on the aerodynamic performance of multiple wind-propulsion systems.

Bouman, E. A., Lindstad, E., Rialland, A. I., and Strømman, A. H. (2017). State-of-the-art technologies, measures, and potential for reducing ghg emissions from shipping – a review. *Transportation Research Part D: Transport and Environment*, 52:408–421.

Carney, J., Cunningham, P., and Bhagwan, U. (1999). Confidence and prediction intervals for neural network ensembles. In *IJCNN'99. International Joint Conference on Neural Networks. Proceedings (Cat. No.99CH36339)*, volume 2, pages 1215–1218 vol.2.

da Silva, I. N., Spatti, D. H., Flauzino, R. A., Liboni, L. H. B., and dos Reis Alves, S. F. (2017). *Artificial Neural Networks - A Practical Course*. Springer International Publishing.

de Kat, J. and Mouawad, J. (2019). Green ship technologies. *Sustainable Shipping*.

EC (2015). Paris agreement. *Climate Action*. `https://climate.ec.europa.eu/eu-action/international-action-climate-change/climate-negotiations/paris-agreement_en`.

EC (2021a). A european green deal. *Green Deal*. `https://commission.europa.eu/strategy-and-policy/priorities-2019-2024/european-green-deal_en`.

EC (2021b). Reducing emissions from the shipping sector. *Climate Action*. `https://climate.ec.europa.eu/eu-action/transport-emissions/reducing-emissions-shipping-sector_en`.

Fam, M. L., Tay, Z. Y., and Konovessis, D. (2022). An artificial neural network for fuel efficiency analysis for cargo vessel operation. *Ocean Engineering*, 264:112437.

Fritz, F. (2013). *Application of an Automated Kite System for Ship Propulsion and Power Generation*, pages 359–372. Springer Berlin Heidelberg, Berlin, Heidelberg.

García, S., Ramírez-Gallego, S., Luengo, J., Benítez, J. M., and Herrera, F. (2016). Big data preprocessing: methods and prospects. *Big Data Analytics*, 1(1):1–22.

Giering, J.-E. and Dyck, A. (2021). Maritime digital twin architecture: A concept for holistic digital twin application for shipbuilding and shipping. *at-Automatisierungstechnik*, 69(12):1081–1095.

GloMEEP (2019). Kite. *GloMEEP - IMO*. `https://glomeep.imo.org/technology/kite/`.

Hermans, J. (2024). Retrofit modeling for green ships. Master's thesis, TU Delft. Report number: MT.23/24.021.M.

Holtrop, J. and Mennen, G. (1982). An approximate power prediction method. *International Shipbuilding Progress*, 29(335):166–170.

Hsu, S. A., Meindl, E. A., and Gilhousen, D. B. (1994). Determining the power-law wind-profile exponent under near-neutral stability conditions at sea. *Journal of Applied Meteorology and Climatology*, 33(6):757 – 765.

Hu, Z., Jin, Y., Hu, Q., Sen, S., Zhou, T., and Osman, M. T. (2019). Prediction of fuel consumption for enroute ship based on machine learning. *IEEE Access*, 7:119497–119505.

IMO (2018). Imo's work to cut ghg emissions from ships. *International Maritime Organization*. https://www.imo.org/en/MediaCentre/HotTopics/Pages/Cutting-GHG-emissions.aspx.

IMO (2021). 2021 guidance on treatment of innovative energy efficiency technologies for calculation and verification of the attained eedi and eex. *International Maritime Organization*.

IMO (2023). 2023 imo strategy on reduction of ghg emissions from ships. *International Maritime Organization*. https://www.imo.org/en/OurWork/Environment/Pages/2023-IMO-Strategy-on-Reduction-of-GHG-Emissions-from-Ships.aspx.

ITTC (2021). Preparation, conduct and analysis of speed/power trials. https://www.ittc.info/media/9874/75-04-01-011.pdf.

Keras (2023). Keras documentation: About keras 3. *Keras*. https://keras.io/about/.

Kiran, D. (2022). Chapter twenty-two - machinery replacement analysis. In Kiran, D., editor, *Principles of Economics and Management for Manufacturing Engineering*, pages 259–267. Butterworth-Heinemann.

Kritzinger, W., Karner, M., Traar, G., Henjes, J., and Sihn, W. (2018). Digital twin in manufacturing: A categorical literature review and classification. *IFAC-PapersOnLine*, 51(11):1016–1022. 16th IFAC Symposium on Information Control Problems in Manufacturing INCOM 2018.

Mauro, F. and Kana, A. (2023). Digital twin for ship life-cycle: A critical systematic review. *Ocean Engineering*, 269.

Mouzakitis, S., Kontzinos, C., Tsapelas, J., Kanellou, I., Kormpakis, G., Kapsalis, P., and Askounis, D. (2023). *Enabling Maritime Digitalization by Extreme-Scale Analytics, AI and Digital Twins: The Vesselai Architecture*, pages 246–256.

Papanikolaou, A., Boulougouris, E., Erikstad, S.-O., Harries, S., and Kana, A. (2024). Ship design in the era of digital transition - a state-of-the-art report. *15th International Marine Design Conference (IMDC 2024)*.

Parkes, A., Sobey, A., and Hudson, D. (2018). Physics-based shaft power prediction for large merchant ships using neural networks. *Ocean Engineering*, 166.

Reche-Vilanova, M., Hansen, H., and Bingham, H. B. (2021). Performance Prediction Program for Wind-Assisted Cargo Ships. *Journal of Sailing Technology*, 6(01):91–117.

Smith, T., Newton, P., Winn, G., and Grech La Rosa, A. (2013). Analysis techniques for evaluating the fuel savings associated with wind assistance.

Stark, C., Xu, Y., Zhang, M., Yuan, Z., Tao, L., and Shi, W. (2022). Study on applicability of energy-saving devices to hydrogen fuel cell-powered ships. *Journal of Marine Science and Engineering*, 10(3).

Swider, A., Wang, Y., and Pedersen, E. (2018). Data-driven vessel operational profile based on t-sne and hierarchical clustering. *OCEANS 2018 MTS/IEEE Charleston*, pages 1–7.

Thies, F. and Ringsberg, J. W. (2023). Retrofitting wasp to a ropax vessel—design, performance and uncertainties. *Energies*, 16(2):673.

van der Kolk, N., Bordogna, G., Mason, J., Bonello, J.-M., Vrijdag, A., Broderick, J., Larkin, A., Smith, T., Akkerman, I., Keuning, J., and Huijsmans, R. (2019). Wind-assist for commercial ships: A techno-economic assessment.

Vigna, V. and Figari, M. (2023). Wind-assisted ship propulsion: Matching flettner rotors with diesel engines and controllable pitch propellers. *Journal of Marine Science and Engineering*, 11(5).

Witzgall, F. (2023). Aerodynamic modelling of wind-assisted ship propulsion. Master's thesis, Institut Supérieur de l'Aéronautique et de l'Espace, Toulouse, France. Thesis completed at French Alternative Energies and Atomic Energy Commission (CEA).